

## Observations of Giant Pulses of the Crab Pulsar \*

Ling-Jun Kong<sup>1,2</sup>, Ali Esamdin<sup>1</sup>, Cheng-Shi Zhao<sup>1,2</sup>, Zhi-Yong Liu<sup>1</sup> and Jian-Ping Yuan<sup>1,2</sup>

<sup>1</sup> Urumqi Observatory, NAOC, Chinese Academy of Sciences, Urumqi 830011, China; [aliyi@uao.ac.cn](mailto:aliyi@uao.ac.cn)

<sup>2</sup> Graduate University of Chinese Academy of Sciences, Beijing 100049, China

Received 2007 August 12; accepted 2007 September 12

**Abstract** The Crab Pulsar was observed at 1540 MHz with the 25m radio telescope at Urumqi with a filterbank de-dispersion backend. A total of 2436 giant pulses with pulse energies larger than  $4300 \text{ Jy } \mu\text{s}$  were detected in two observing sets. All of these giant pulses are located in the main pulse (MP) and inter pulse (IP) windows of the average profile of the Crab Pulsar. The ratio of the numbers of giant pulses detected in the IP and MP windows is about 0.05. Our results show that, at 1540 MHz, the emission in the IP is contributed by giant and normal pulses, while that in the MP is almost dominated by giant pulses. The distribution of energy of the 2436 giant pulses at 1540 MHz can be described by a power-law with index  $\alpha = 3.13 \pm 0.09$ . The intrinsic threshold of giant pulse energy in the MP window is about  $1400 \text{ Jy } \mu\text{s}$  at 1540 MHz.

**Key words:** stars: neutron — pulsars: general — pulsars: individual Crab Pulsar

### 1 INTRODUCTION

Giant pulses are a special and most striking form of pulsar radio emission with durations much shorter than the so-called subpulses. Giant pulses from Crab Pulsar were first detected before it was identified as a pulsar completely (Staelin & Reifenstein 1968), they typically have durations from several microseconds down to a few nanoseconds. Hankins et al. (2003) found the giant pulse structure of Crab Pulsar to be as short as 2 ns. Some previous research indicated that the giant pulses are only found in the main and inter pulse windows of Crab Pulsar at lower frequency (Lundgren et al. 1995; Sallmen et al. 1999; Cordes et al. 2004) while Slowikowska et al. (2007) noted giant pulses at nearly all phases of the Crab Pulsar at frequency 8.35 GHz.

The average pulse profile is constructed by averaging thousands of successive individual pulses. The average profile of the Crab Pulsar at 1540 MHz consists of two main components: an intense but narrow ‘main pulse’ (MP), and a broader and weaker ‘inter pulse’ (IP) following the MP by 13.37 milliseconds. The phase separation between the MP and the IP is  $\sim 0.4$ . At lower radio frequencies (300–600 MHz), another broad and weak component is visible. It precedes the MP by 1.6 milliseconds (about  $17.5^\circ$ ) and is called a ‘precursor’ (P), but in the average pulse profile at 1.4 GHz, the precursor vanishes, leaving only MP, IP and a weak but distinct low frequency component (LFC), which is  $\sim 36$  degrees ahead of the MP, but not coincident with the position of the precursor apparent at the lower frequency (Moffett & Hankins 1996). Cordes et al. (2004) pointed out that the detection efficiency of giant pulse in 1.4 GHz is about 0.31 per second, i.e. 1 giant pulse in 3.3 s. The distribution of flux densities of giant pulses is in the power law (Argyle & Gower 1972; Cordes 1976; Lundgren et al. 1995).

We observed the Crab Pulsar at 1540 MHz by using the Urumqi 25m radio telescope. The details of the observations are given in Section 2. In Section 3, the data reduction process and some results are presented. A discussion and some conclusions are given in Section 4.

---

\* Supported by the National Natural Science Foundation of China.

## 2 OBSERVATIONS

Observations were conducted at 1540 MHz on 2007 May 19 (MJD 54239). A total of 2.66 hours of data were obtained in two observational runs. A dual-channel cryogenic receiver system sensitive to two orthogonal linear polarizations was used. The center frequency of each receiver is 1540 MHz, with a bandwidth of 320 MHz. The noise temperature of the receiver is less than 10 K. The signals were down-converted to the intermediate frequency (IF) with a range of 240 MHz in the local oscillator (LO). Then, the signals of IF were de-dispersed with a filterbank system having 128 sub-channels on each of the two orthogonal linear polarizations. The data were then recorded on a disk with 1-bit sampling. The details of observation and recording system can be found in Wang et al. (2001). The sensitivity of receiver is

$$S_{\min} = \frac{2kT_{\text{sys}}}{\eta A^2 \sqrt{n_p \tau \Delta f}}, \quad (1)$$

where  $k$  is the Boltzmann's constant,  $T_{\text{sys}}$  the total system temperature at 1540 MHz,  $\eta$  the efficient of the antenna at 1540 MHz,  $A$  the area of antenna,  $n_p$  the number of polarization,  $\tau$  the sampling time and  $\Delta f$  the total bandwidth.

When observing the Crab Pulsar, the total system temperature is defined by

$$T_{\text{sys}} = T_{\text{R}} + T_{\text{bg}} + G \times I_{\text{CN}}, \quad (2)$$

where  $T_{\text{R}}$  and  $T_{\text{bg}}$  are temperatures produced by radiometer noise and background sky radiation, respectively.  $G$  is the telescope gain,  $I_{\text{CN}}$  is the flux density of the Crab Nebula which can be approximated by the relation  $I_{\text{CN}} = 955\nu^{-0.27}\text{Jy}$  ( $\nu$  in GHz) (Allen 1973; Bietenholz et al. 1997). As for the observations of the Crab Pulsar at 1540 MHz with the Urumqi telescope,  $T_{\text{R}} + T_{\text{bg}}$  is equal to 22 K,  $G \times I_{\text{CN}}$ , 86.2 K;  $\eta$ , 57%;  $A$ , 490.87 m<sup>2</sup>;  $N_p$ , 2;  $\tau$ , 0.25 ms; and  $\Delta f$ , 320 MHz; so the sensitivity of the system at 1540 MHz is 2.667 Jy.

To increase the sensitivity of observation, we enlarged the bandwidth of the receiver. Due to the dispersion caused by the interstellar medium (ISM), the velocity of the radio wave is frequency-dependent, i.e., it is faster at high than low frequencies. This will broaden the pulse width and reduce the peak flux density. The broadening of the pulse is given by

$$W = W_{50} + \Delta t_{\text{DM}} + t_{\text{scatt}}, \quad (3)$$

where  $W_{50}$  is the initial width of pulse before the broadening,  $\Delta t_{\text{DM}}$  is the pulse dispersion broadening due to the sub-channel bandwidth, and

$$\text{DM} = \int n_e dl, \quad (4)$$

$$\Delta t_{\text{DM}} = (8.3\mu\text{s})\text{DM}\Delta\nu_{\text{MHz}}\nu_{\text{GHz}}^{-3}. \quad (5)$$

In Equation (3),  $t_{\text{scatt}}$  is the pulse broadening due to the interstellar scattering. Popov et al. (2006a) pointed out that the scattering broadening of the pulse is given by

$$t_{\text{scatt}} = 20(\nu_{\text{MHz}}/100)^{-3.5}(\text{millisecond}). \quad (6)$$

Equation (5) shows that the pulse dispersion broadening due to the ISM is proportional to the dispersion measure (DM) and the bandwidth of the channel, and is inversely proportional to the frequency cubed. The DM is proportional to the average electron density of ISM and the distance between the pulsar and the observer. Equation (6) shows that the pulse scatter-broadening is proportional to  $\nu_{\text{MHz}}^{-3.5}$ . So the dispersion broadening and scattering broadening can be reduced by observing at higher frequencies.

For the observations of Crab Pulsar with the Urumqi system, the DM is 56.791 cm<sup>-3</sup> pc, the central frequency 1540 MHz, and the bandwidth of each sub-channel 2.5 MHz, so the dispersion broadening for each sub-channel is  $\Delta t_{\text{DM}} = 0.323$  ms, and the scatter-broadening is about 1.40  $\mu\text{s}$ . Assuming, for the giant pulses of Crab Pulsar,  $W_{50}$  is about 1  $\mu\text{s}$ , the pulse width will be broadened to about 0.325 ms. Now our sampling time is 0.25 ms, so such giant pulses can be detected. For a signal-to-noise ratio  $S/N = 5$ , the peak flux density of the pulse is about 13.335 Jy and the minimum energy which can be detected is about 13.335 Jy  $\times$  0.325 ms, so the Urumqi system can respond to giant pulses with energies greater than 4300 Jy  $\mu\text{s}$ .

### 3 DATA REDUCTION AND RESULTS

#### 3.1 Identification of Giant Pulses from the Crab Pulsar

Identification of observed giant pulses is a key step in our investigation. Although the pulses are broadened by dispersion and scattering, the giant pulses are still narrow, and can only be described by 3~4 sample points in our observations. The characteristics of the giant pulse radiation and the propagation effect of pulse signals in interstellar medium are used to identify the giant pulses.

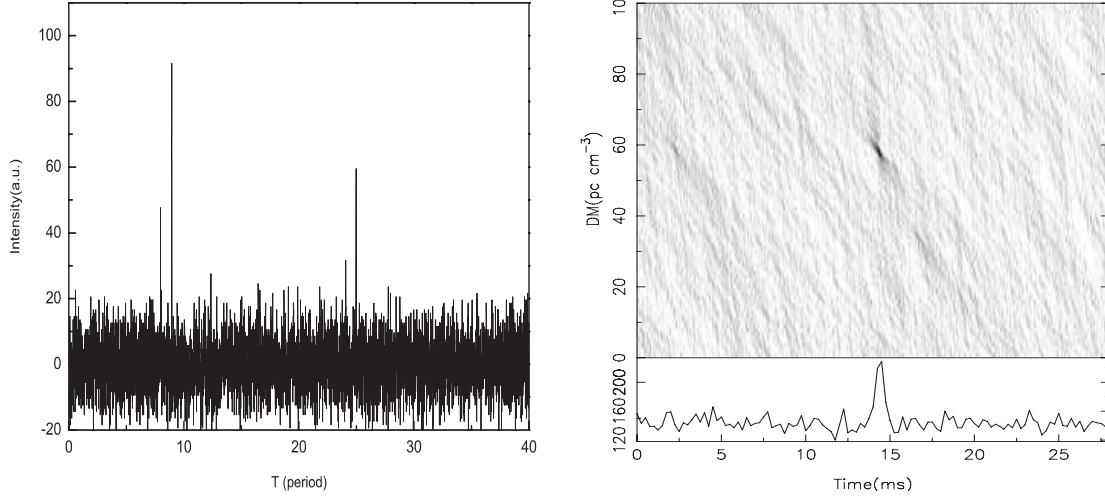


**Fig. 1** Typical giant pulses detected in 40 pulse periods (left) and DM signal searching of the second giant pulses (right).

First, we perform de-dispersion to 256 channel data at dispersion measure  $DM = 56.791 \text{ cm}^{-3} \text{ pc}$  to pick out all the signals with signal-to-noise ratios  $S/N \geq 5$ . Secondly, in order to verify that the observed signals come from the pulsar, we need to perform de-dispersion to all the signals selected by using the DM signal searching program. The value range of de-dispersion DM is from 0 to  $100 \text{ cm}^{-3} \text{ pc}$  and the searching step is  $1 \text{ cm}^{-3} \text{ pc}$ . With this method, we can analyze the evolution of the signal intensity and width with the DM, and distinguish noise from the giant pulse signal. In order to use weak signals, we choose a short step,  $0.1 \text{ cm}^{-3} \text{ pc}$ .

The left panel of Figure 1 shows three giant pulses in 40 successive pulses obtained after performing the de-dispersion at  $DM = 56.791 \text{ cm}^{-3} \text{ pc}$ . The right panel shows the DM signal searching diagram. The searching range is from  $0 \sim 100 \text{ cm}^{-3} \text{ pc}$  and the searching step is  $1 \text{ cm}^{-3} \text{ pc}$ . A total of 2436 giant pulses were identified by using this method from the two sets of observed data.

The state of the observational system affects the detection efficiency. In a continuous observation of 2.66 hours, our detection efficiency is 1 giant pulse in 120 pulse periods. This is very close to the result presented by Cordes et al. (2004).

#### 3.2 Phase of the Giant Pulses

An average profile is obtained by folding all individual pulses in the two datasets we used. Then the phase of each giant pulse in the average profile is fixed. The folding period is calculated by using the JODRELL BANK CRAB PULSAR MONTHLY EPHEMERIS (<http://www.jb.man.ac.uk/research/pulsar/crab.html>) published in March 2007 by the Jodrell Bank Observatory. Considering that there may be relatively large timing irregularities in the duration between our observations and the ephemeris, we test the folding period by randomly distributed giant pulses in two datasets, which can improve the veracity of the giant pulse phase.

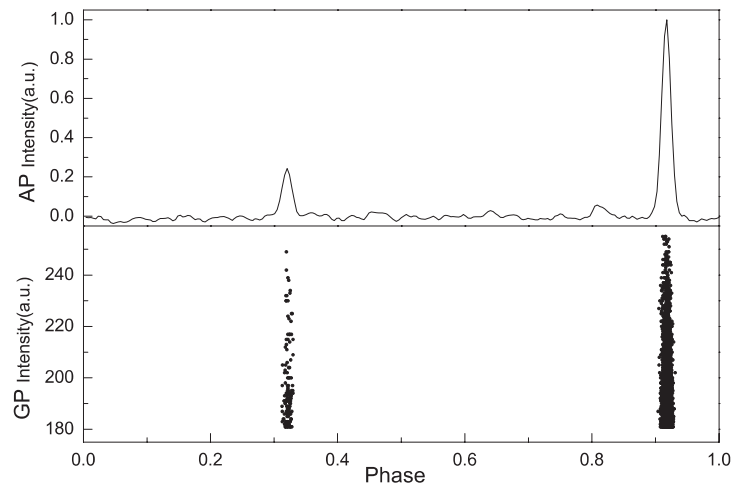


**Fig. 2** Average profile obtained from all 2.66-hour data (upper) and the distribution of 2436 giant pulses (lower). The units of intensity in the two panels are arbitrary.

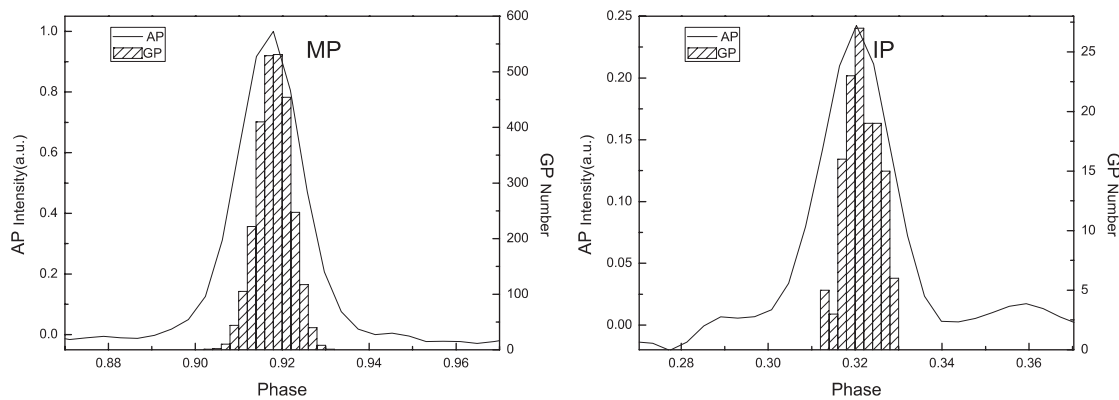


**Fig. 3** Accumulative phase distribution (in bar graph) of giant pulses in MP windows (left) and IP window (right). The units of intensity in the two panels are arbitrary.

The average profile of Crab Pulsar contains different components in different frequencies other than the MP and IP. Figure 2 shows the average profile we obtained by overlapping all individual pulses at 1540 MHz (upper) and the distribution of the 2436 giant pulses (lower). The average profile shows three components: MP, IP and a weak low frequency component (LFC). The phases of IP, LFC and MP in Figure 3 are 0.32, 0.808 and 0.918, respectively. Although LFC has been detected in 800 MHz and 1400 MHz, there are no LFC observed in 600 MHz and below. However, there is a component, a leading component of MP at the lower frequency, labelled P in Moffett & Hankins (1996).

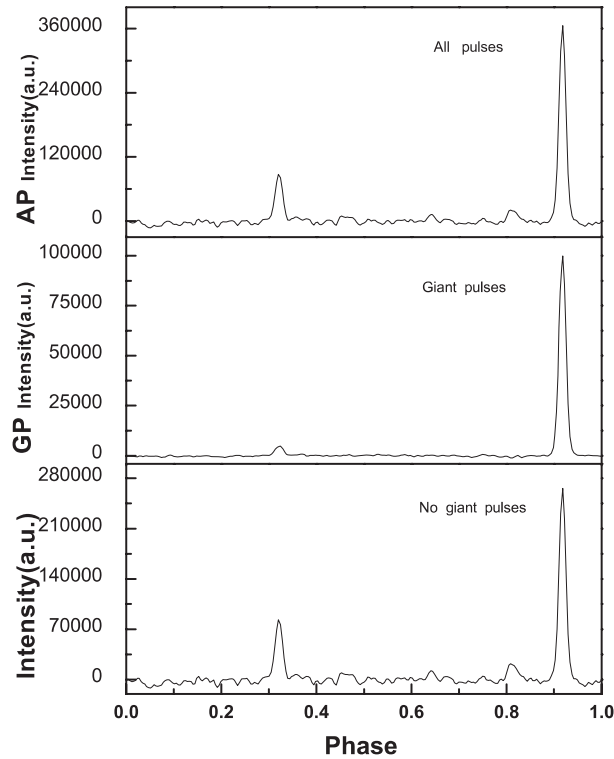
Figure 2 shows that all the giant pulses are located in the narrow windows of the MP and IP, and no giant pulses detected in LFC. A more detailed statistics shows that there are 113 giant pulses detected in the IP window and 2323 in the MP window, and the ratio of the two ( $N_{IP}/N_{MP}$ ) is about 0.05.

Figure 3 presents the accumulative phase distribution of giant pulses in MP and IP. It shows that the phase distribution of giant pulses in the MP and IP windows is similar to that of the energy distribution. This result is consistent with that of Cordes et al. (2004). Figure 3 also shows that the distribution of giant

pulses lags a bit in the windows of MP and IP, especially in the MP window. This needs to be confirmed by further observations.

### 3.3 The Average Profile of Giant Pulses

Figure 4 presents the average profile of all individual pulses from the two datasets (upper panel) and the average profile produced by all the 2436 giant pulses detected (middle panel). Although the number of giant pulses is much smaller than that of all individual pulses ( $2436 \ll 284429$ ), the average giant pulse profile has a greater signal-to-noise ratio, which indicates significant contribution of giant pulses to average profile of the Crab Pulsar.



**Fig. 4** Average profiles of all individual pulses (upper) and that of 2436 giant pulses (middle), and profile produced by individual pulses without giant pulses (lower).

The average profiles produced by all giant pulses and all pulses (middle and upper panels of Fig. 4, respectively) show that the ratio of energy from the MP of the middle panel to that of upper panel is 0.28, while that of IP is 0.06, so the giant pulses make a greater contribution to the MP component than to the IP component. We note that the width of the MP in the average profile of all giant pulses (0.58 ms) is appreciably wider than that of all pulses (0.56 ms) at 1540 MHz.

The lower panel of Figure 4 shows the average profile of all individual pulses without contributions of giant pulses. This figure makes the LFC much more prominent than does the result obtained in the same frequency by Moffett & Hankins (1996). The LFC leads by 18.5 degree to the P component observed in the lower frequency (300 ~ 600 MHz) by Moffett & Hankins (1996). The P component has a wider window than the LFC. Furthermore, the intensity ratio of IP and MP gets greater after subtracting the giant pulses. These facts suggest that the normal pulses form the LFC and normal pulses contribute more to the IP than that to the MP.

Comparing the MP in the lower panel with that in the middle panel, we obtain the ratio ( $R$ ) between the intensity of MP in the profile of no giant pulse contribution (lower panel) and that in the profile of all giant pulses,  $R = 2.66$ .

### 3.4 The Probability Distribution of Energy of Giant Pulses

The probability distribution (PD) of the energy of giant pulses is

$$\text{PD} = KE^{-\alpha}, \quad (7)$$

where  $E$  is the average pulse energy,  $\alpha$  the spectral index. Previous research showed that the spectral index is in the range 2.1 – 3.4 for different frequencies for the Crab Pulsar (Argyle & Gower 1972; Lundgren et al. 1995; Jessner et al. 2005).

The energy of the giant pulse was calculated with the equation of  $E = S \times W_{50}$ . The peak flux density  $S$  is proportional to the S/N of the pulse. The initial width of the giant pulse is very narrow, from several microseconds down to few nanoseconds. In Section 2, we showed that the broadened giant pulse is thousands times wider than its initial width. Because of this, all the broadened pulses in our observations have nearly the same width. So the histogram of giant-pulse S/N could be taken to denote the probability distribution (PD) of giant pulse energy.

Figure 5 shows the S/N for all the 2436 giant pulses detected with  $S/N \geq 5$  at 1540 MHz. The results from the previous investigations suggest that, unlike the normal pulses, the distribution of giant-pulse amplitudes is characterized by power laws (e.g., Argyle & Gower 1972; Lundgren et al. 1995). Likewise, our histogram of giant-pulse S/N for 2436 giant pulses shows the same form of power law distribution. By fitting to a power law (Fig. 5), we obtained a power law index of  $\alpha = 3.13 \pm 0.09$ . As shown in Figure 5, there is slightly deviation to the fit in the region of high S/N (about  $> 12$ ), very possibly because of insufficient statistics of high energy giant pulses.

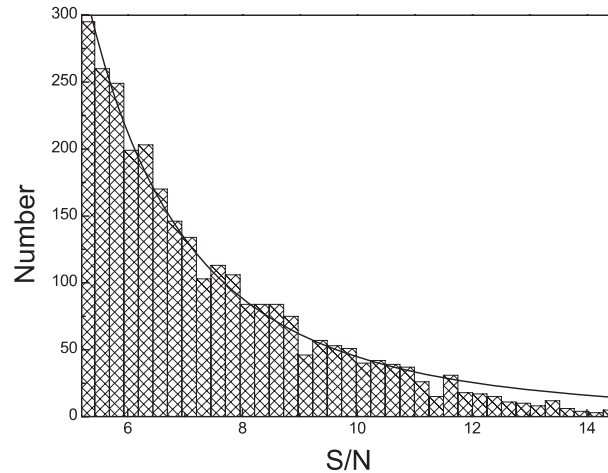


**Fig. 5** Distribution of the S/N of 2436 giant pulses and the fitting with a spectral index of  $\alpha = 3.13 \pm 0.09$ .

## 4 DISCUSSION AND CONCLUSIONS

Lundgren et al. (1995), Sallmen et al. (1999) and Cordes et al. (2004) noted that the giant pulses from the Crab Pulsar occur exclusively in the MP and IP windows, while Knight (2007) found that the giant pulses from PSR J1823–3021A coincide with the ordinary emission phases. The LFC in the average profile of Crab Pulsar was detected in our observations at 1540 MHz. All 2436 giant pulses in the two datasets are located in the MP and IP windows but no giant pulse is detected in LFC phase range, so our results support the former investigations. The ratio of the number of giant pulses detected in IP and MP windows at 1540 MHz is about 0.05, which is consistent with the result obtained at 1475 MHz by Cordes et al. (2004).

The giant pulses emitted by the millisecond pulsar B1937+21 are located in the trailing edges of both the MP and IP of its regular profile (Cognard et al. 1996; Kinkhabwala et al. 2000; Soglasnov et al. 2004). Popov et al. (2006) pointed out that there is no giant pulses in the P component at 600 MHz, and suggested that the MP may be a trailing component of the P component. Both Popov et al. (2006) and Friedman & Boriakoff (1992) suggested that there might be a P component, leading the IP windows of Crab Pulsar. If these views are correct, the location of giant pulses from the Crab Pulsar is consistent with that from the millisecond pulsar B1937+21. However, no observations showed P component of IP up to now and we did not detect any giant pulse in LFC. We suggest that the LFC in our observations and the P component at lower frequency may be the same component, but with a large phase shift within the frequency range between 600 MHz and 1400 MHz. Further multi-frequency observations are needed to confirm this suggestion.

Some of the previous work on fitting the PD or the cumulative probability distribution (CPD) of the energies of giant pulses, have used either the spectrum index  $\alpha$  or  $\gamma$ , with  $\gamma = \alpha - 1$ . Popov et al. (2006) derived that the index of CPD fitting for the energies of giant pulses is 2.2 at 600 MHz, while Jessner et al. (2005) gave a PD index of 3.34 at 8.35 GHz by fitting the peak flux density of giant pulses. These two values are close to our value derived for 1540 MHz. Popov et al. (2006) noted a lower limit of peak flux density of giant pulses in the MP window of 105 Jy at 600 MHz. Using the equation  $E_{\text{thresh}} = E_{\text{lim}}(R + 1)^{1/(2-\alpha)}$  (Popov et al. 2006b), we obtain that the intrinsic threshold of energy of giant pulses in MP window is about 1400 Jy  $\mu\text{s}$  at 1540 MHz, where  $E_{\text{thresh}}$  is the intrinsic threshold for giant pulses,  $E_{\text{lim}} = 4300 \text{ Jy } \mu\text{s}$  is the minimum energy of detected giant pulses in this work,  $R = 2.66$ , as presented in Subsection 3.3, and the PD fitting index  $\alpha = 3.13$ .

We have arrived at conclusions as follows:

1. In our two datasets, all the giant pulses are located in the MP and IP windows, and the ratio of the numbers in IP and MP windows is about 0.05. The giant pulses contribute more to MP component than that to IP at 1540 MHz. A significant fraction of energy in IP comes from normal pulses.
2. LFC is detected in the average profile of the Crab Pulsar at 1540 MHz, in the range  $30 \sim 40$  degrees ahead of the MP, and is produced by normal pulses without giant pulse contribution. This is consistent with the P components at a lower frequency. We suggest that the LFC and P component at the lower frequency have the same origin, and the phase difference might be due to the evolution of component phase with frequency.
3. The minimum giant pulse energy in our observations is about 4300 Jy  $\mu\text{s}$ . A power law fitting to the probability distribution of the energies of the 2436 giant pulses gives a spectral index of  $\alpha = 3.13 \pm 0.09$ . Under the assumption that the giant pulse energy follows the power-law down to a certain threshold, we suggest that the intrinsic threshold of energy of giant pulses in the MP window is about 1400 Jy  $\mu\text{s}$  at 1540 MHz.

**Acknowledgements** The authors thank M. V. Popov and H. S. Knight for helpful comments. This work was supported by the National Natural Science Foundation of China (NSFC) under No.10573026, the program of the Light in China's Western Region (LCWR) under No. LHXZ200602, and the Key Directional Project of CAS.

## References

- Allen C. W., 1973, *Astrophysical quantities* (University of London. Athlone Press)
- Argyle E., Gower J. F. R., 1972, *ApJ*, 175, L89
- Argyle E., Gower J. F. R., 1972, *BAAS*, 4, 216
- Bietenholz M. F., Kassim N., Frail D. A. et al., 1997, *ApJ*, 490, 291
- Cognard I., Shrauner J. A., Taylor J. H. et al., 1996, *ApJ*, 457, L81
- Cordes J. M., Bhat N. D., Hankins T. H. et al., 2004, *ApJ*, 612, 375
- Gower J. F. R., Argyle E., 1972, *ApJ*, 171, L23
- Friedman J. F., Boriakoff V., IAU Coll. 128 Univ. Press, Poland, 1992, 374
- Hankins T. H., Kern J. S., Weatherall J. C., Eilek J. A., 2003, *Nature*, 422, 141
- Jessner A., Slowikowska A., Klein B. et al., 2005, *AdSpR*, 35, 1166
- Knight H. S., 2007, *MNRAS*, 378, 723

- Kinkhabwala A., Thorsett S. E., 2000, *ApJ*, 535, 365  
Kuzmin A. A., 2006, *Chin. J. Astron. Astrophys. (ChJAA)*, 6S2, 34  
Lundgren S. C., Cordes J. M., Ulmer M. et al., 1995, *ApJ*, 453, 433  
McLaughlin M. A., Lyne A. G., Lorimer D. R. et al., 2006, *Nature*, 439, 817  
Moffett D. A., Hankins T. H., 1996, *ASPC*, 105, 283  
Popov M. V., Kuz'min A. D., Ul'yanov O. M. et al., 2006a, *Astronomy Reports*, 50, 562  
Popov M. V., Soglasnov V. A., Kondrat'Ev V. I. et al., 2006b, *Astronomy Reports*, 50, 55  
Sallmen S., Backer D. C., Hankins T. H. et al., 1999, *ApJ*, 517, 460  
Shearer A., Stappers B., O'Connor P. et al., 2003, *Science*, 301, 493  
Slowikowska A., Jessner A., Kanbach G. et al., 2007, eprint arXiv:astro-ph/0701105  
Soglasnov V. A., Popov M. V., Bartel N. et al., 2004, *ApJ*, 616, 439  
Staelin D., Reifenstein E. C., 1969, *Science*, 162: 1481  
Wolszczan A., Cordes J., Stinebring D., 1984, *bens. Work*, 63  
Wang N., Manchester R. N., Zhang J. et al., 2001, *MNRAS*, 328, 855